

Chapter 8

Laser-Plasma Particle Sources for Biology and Medicine

Antonio Giulietti, Giancarlo Bussolino, Lorenzo Fulgentini,
Petra Koester, Luca Labate and Leonida A. Gizzi

Abstract Ultrashort, intense laser pulses can drive in plasmas small sized linear accelerators (Laser-Linac's) of high energy elementary particles. These novel devices are facing a continuous, fast progress making them suitable alternatives to conventional linacs in many applications. Among them, cancer therapy may have by far the highest social impact at a global level. This paper is aimed at giving an updated overview of the scientific and technological effort devoted worldwide to the optimization of the laser acceleration technology in order to fulfill the clinical requirements. Here we discuss both ion and electron acceleration considering the different, challenging problems to be solved in each case. Current studies on radiobiology already in progress in many labs with the existing laser-based sources of particles are also described. The overall scenario in the field appears extremely exciting, and promises rapid, effective development.

A. Giulietti (✉) · G. Bussolino · L. Fulgentini · P. Koester · L. Labate · L.A. Gizzi
Intense Laser Irradiation Laboratory, Istituto Nazionale di Ottica,
CNR Campus, via Moruzzi, 56124 Pisa, Italy
e-mail: antonio.giulietti@ino.it

G. Bussolino
e-mail: giancarlo.bussolino@ino.it

L. Fulgentini
e-mail: lorenzo.fulgentini@ino.it

P. Koester
e-mail: petra.koester@ino.it

L. Labate · L.A. Gizzi
INFN, Sezione di Pisa, Italy
e-mail: luca.labate@ino.it

L.A. Gizzi
e-mail: leonidaantonio.gizzi@ino.it

8.1 Introduction

High-field photonics [1] is one of the most exciting branches of ultrashort intense laser science. Powerful femtosecond lasers, coupled with suitable focusing optics, can shoot into matter optical “bullets” whose transverse size (the spot size) is comparable with the longitudinal size (the pulse length) and whose photon density is of the order of 10^{27} phot/cm³. The oscillating electric field in the bullet volume can exceed 10^{12} V/cm, much higher than atomic fields. When interacting with matter, such pulses are able to ionize atoms in a time of the order of a single optical cycle, i.e. in a fs or less. Free electrons are then moved by the oscillating electric field to relativistic quiver velocities, so opening the novel field of investigation commonly referred to as *optics in the relativistic regime* [2].

In this framework, we can roughly distinguish between two levels of laser intensity. At a lower level, the electric field can be just comparable with the one requested for the ionization of the medium. This condition produces a strong modification of the laser pulse parameters, including the oscillation frequency of the e.m. field. This case has been studied by several authors. In particular, Le Blanc et al. [3] reported one of the first clear observations of spectral blue shifting of a femtosecond laser pulse propagating in a dense gas. Interestingly, a well defined spectral shift was also measured after anomalous propagation in an overdense plasma slab [4]. A number of papers report on spectral effects in conditions of interest for laser driven electron acceleration. Koga et al. observed blue shift up to 40–50 nm, which was attributed to a combined effect of ionization and filamentation [5]. Giulietti et al. observed 25 nm peak blue shift with modulated spectral tails extending up to 100 nm, mostly attributed to self-phase modulation [6]. Recently [7], observation of extreme blue shifting has been reported for a 65-fs, 800-nm, 2-TW laser pulse propagating through a nitrogen gas jet, experimentally studied by 90° Thomson scattering. Time-integrated spectra of scattered light show unprecedented broadening towards the blue which exceeds 300 nm. Images of the scattering region provide for the first time a space- and time-resolved description of the process leading quite regularly to such a large upshift. The mean shifting rate was as high as $d\lambda/dt \approx 3 \text{ \AA}/\text{fs}$, never observed before. In principle this effect allows the spectrum of ultrashort laser pulses to be shifted and tuned, with possible applications in many fields. It has to be noticed that relevant laser frequency shifts due to ultrafast ionization are in general observed at intensity below the one suitable for laser acceleration. In particular the extreme shift described in [7] was observed in an acceleration experiment but during the late propagation of the laser pulse in a gas jet, when its intensity had been reduced by energy depletion and beam defocusing.

At higher laser intensities, ionization time is much shorter than the usual pulse duration (a few tens of femtoseconds) and almost all the pulse propagates in a fully ionized medium. In this condition the e.m. field is able to excite, via ponderomotive displacement in a plasma of suitable density, electron waves of very large amplitude, whose longitudinal electric field has the typical properties of an accelerator cavity, able to accelerate free electrons up to relativistic kinetic energies. The suitable plasma

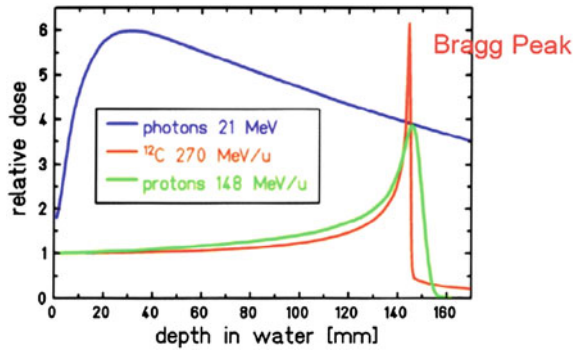
density depends on the regime of acceleration chosen but usually the plasma working density is well below the critical density $n_c = (m_e/4\pi e^2)\omega_L^2$, where e and m_e are electron charge and mass respectively, ω_L is the laser light pulsation. Local acceleration fields in these electron plasma waves are at least 3 orders of magnitude higher than in the cavities of Radio-Frequency driven ordinary Linacs. This means for example that multi-MeV electrons can be produced in a millimetric laser path rather than in meter-long RF cavity. A striking feature of the laser-produced electron bunches is their ultrashort duration, typically of the order of 1 ps, more than 10^6 times shorter than bunches produced with RF technology. Possible relevant consequences of this feature will be discussed below.

Since the original idea of Laser Wake-Field Acceleration [8] and the advent of the decisive CPA laser technology [9], a number of schemes for laser driven acceleration of electrons in plasmas have been proposed and studied, some of which were successfully tested. New experimental records have been reported in the recent literature, in terms of the maximum electron energy achieved, the minimum energy spread, as well as maximum collimation, stability, and so on. These records are in general obtained with lasers of outstanding performances and/or with very sophisticated methods hardly applicable for practical uses. On the other hand, many labs are intensively working on scientific and technological innovations aimed at demonstrating that reliable laser-based devices can be built which are able to produce electron beams fulfilling requirements of specific applications. A major task is addressed to the possible clinical use of electron Laser linacs and their potential advantages with respect to the existing RF-linacs operating today for millions of daily hospital treatments in the world.

Laser driven electron acceleration through excitation of plasma waves acts on free electrons already available in a plasma. In general the primary interaction of the laser field is with electrons (either bound or free), while action on massive particles (protons and ions) needs the intermediate role of electrons. For this reason, though evidence of the effect of the laser field on the ion velocity was found as early as high power lasers entered the laboratory, the first relevant effects on ion acceleration were observed, in the fusion research context, with powerful CO₂ lasers [10, 11]. These latter in fact, due to their large wavelength (10- μ m) can induce huge electron quiver velocities on plasma electrons.

Historically, ion acceleration in plasmas was proposed before the invention of optical lasers, as early as 1956 [12] and initially tested with electron beams propagating in plasmas. Apart from initial observation related to fusion studies with infrared CO₂ lasers cited above, the laser driven ion acceleration studies with optical lasers could really start only after some decisive breakthrough towards high peak power lasers, like mode-locking (ML) for picosecond pulses and chirped pulse amplification (CPA) for femtosecond pulses [9]. About 1-MeV ions were produced in the early Nineties with picosecond laser pulses [13]. Since then, an impressive progress towards higher kinetic energies was continuously driven by both innovation in laser technology and better comprehension of the complex physics involved in the ion acceleration processes. Several proposals raised for a variety of schemes of laser-matter interaction at ultra-high (ultra-relativistic) intensities able to drive protons and

Fig. 8.1 Relative dose deposition versus depth in water for three kinds of ionizing agents, each one with a specific energy



light ions to near-relativistic energies. Most of them can be attributed either to *target normal sheath acceleration* (TNSA) or *radiation pressure dominated acceleration* (RPDA), shortly described in Sect. 2.2.

Also in the case of protons/ions accelerated with laser-based techniques, clinical applications (chiefly hadron-therapy of deep tumors) are a major objective, considering the peculiar character of energy deposition of hadrons in a medium. Figure 8.1 clearly shows that, treating a tumor at 15 cm depth, monoenergetic protons and Carbon ions of suitable kinetic energy deliver most of the dose in a thin layer (Bragg peak) around the tumor site, while monochromatic gamma-rays leave a lot of energy inside healthy tissues before and after the tumor with possible damages on these latter tissues. This drawback has been strongly reduced with modern configurations allowing multi-beam irradiations at different angles. It has to be considered that gamma-ray (or hard X-ray) treatments are still more than 95 % of the current treatments worldwide, while hadron therapy is limited due to the size and cost of proton/ion accelerator plants. That is why laser-based techniques of acceleration have been indicated quite early as a possible way to access hadron treatment of cancer with reduced cost and plant size [14].

In general, considering the present state of the art, we can say that laser-driven acceleration to kinetic energies suitable for radiotherapy of cancer is well consolidated in the case of electrons and bremsstrahlung photons (with bunches delivering the requested dose). Effort is being invested towards achievement of corresponding energies for protons and light ions. Time for technological and commercial alternative with existing Hospital electron-Linac's as well as with rare, huge plants already operating hadron therapy, may not be so far. In the case of electrons most of the work to be done, in order to achieve clinical standards, has to address the control of the electron energy, as well as stability and reliability of the laser-linac. In the case of protons and light ions the work to be done still includes the identification of an acceleration regime able to produce particles of suitable energy and energy spread in bunches delivering the right dose.

However, there is a major scientific issue which has to be addressed from now, concerning potential radiobiological effects of the extremely different duration of

bunches produced by laser with respect to bunches produced by conventional accelerators. A factor exceeding 1,000,000 is involved, from μs to sub-ps timescale. The ultrashort duration of laser-produced particle bunches may involve unexpected consequences for cancer therapy. In fact, it is not known if delivering the same dose with particles of the same kinetic energy but at much higher instantaneous dose-rate may lead to a different tissutal effects with possible consequences on therapeutic strategy and protocols [15]. From the physical point of view we can expect that the extreme particle density we can produce in a bunch with laser acceleration could produce some “collective effect” which cannot be described by the usual single-particle Monte Carlo simulation. In other words it is possible that each ultradense bunch of electrons could produce not only the statistic sum of the effects of each low-LET particle but also some high-LET effect due to the total charge involved. If this would be true, the biological action could not only concern DNA but also some structural cellular feature, like membrane. This major issue, in turn, calls for a dedicated research on radiobiological effects to be performed with the ultrashort particle bunches produced by laser technology. It is evident that such a research also has a high conceptual value since it enables, for the first time, the investigation of very early processes occurring in the timescales of physical, chemical, biological responses of the living matter to ionizing radiation [16].

In this work we will give a concise description of the state of the art and perspectives of the laser technologies currently being developed to address implementation of compact particle accelerators for biological research and clinical uses. Section 8.2 will be devoted to laser-based hadron acceleration and their use in radiobiology with an evaluation of their progress in the perspective towards radiotherapy of tumors. Need of upgrading existing lasers will be also considered. Section 8.3 will shortly describe different kinds of presently available laser Linac’s with particular attention to the clinical requirements, efficiency and reliability of the devices. Interest to sub-relativistic electron sources will also be discussed. In Sect. 8.4 we will consider the main features of radiobiology with laser-plasma electron source, including dosimetry, in vivo tests and numerical simulations. Possibility of investigating very early effects arising from ultrashort ionizing pulses at nanometric scale will be discussed.

8.2 Radiobiology with Protons and Ions from Laser-Based Sources

8.2.1 Present RF-Driven Versus Future Laser-Driven Devices (Protons and Ions)

Considering the great advantages of hadron therapy and the fast progress in laser-based techniques, about 10 years ago, a few interesting and detailed proposals were published for using laser-driven hadron accelerators in medicine for radiological treatment of cancer [14, 17]. These proposals were strongly motivated by the huge

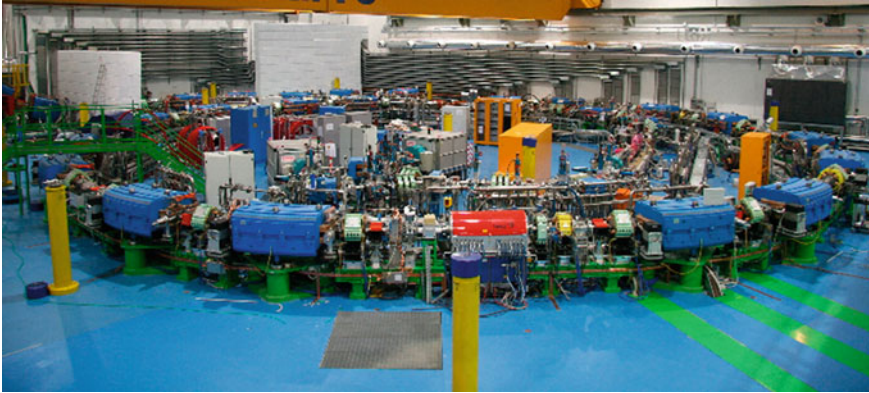


Fig. 8.2 Overview of the CNAO synchrotron, Pavia, Italy

size and cost of present conventional ion accelerators, mostly cyclotron and synchrotron devices, few tens of which are operating nowadays worldwide in a clinical background. As an example, Fig. 8.2 shows the overview of the Centro Nazionale di Adroterapia Oncologica (CNAO) synchrotron operating for clinical use in Pavia (Italy) [18]. Interesting information on principles of proton-therapy and treatment options in the advanced Northeast Proton Therapy Center (Boston, USA), can be found in [19].

After the first proposal for using hadron particles for radiotherapy of cancer [20] and several pioneering experimental tests [21], hadron therapy was occasionally performed inside accelerator facilities devoted to high energy physics, until the opening (1990) of a first clinical center equipped with a proton accelerator facility at Loma Linda Hospital in California (USA). Since then, the number of similar centers grew regularly year by year worldwide with a huge capital investment. The most important facilities operating in the year 2011 are listed in Table 8.1, in the order of their opening year.

Though RF-based devices have faced an impressive progress, mostly in the synchrotron configuration [22], typical acceleration gradients remain of the order of 1MeV/m, so that the typical diameter of an accelerator ring is several tens of meters for energies of clinical interest, namely $E \approx 100\text{--}400$ MeV/u, with severe costs involved [23]. Additional high costs and large spaces are requested by the very heavy gantry systems necessary to guide the particle beam onto the patient body from the right direction(s) and focus it with a millimeter precision [24].

With such a strong motivation, research on laser-based proton acceleration has been considerably supported in the last decade, mostly in the direction of achieving the challenging performances requested by the clinical standards. According to Fig. 8.1 and Table 8.1, we can see that a usable device for cancer therapy needs to produce 200–250 MeV protons and/or 400–450 MeV/u carbon ions. In order to really profit of the Bragg peak, no more than 1 % energy bandwidth is requested. Further, to release a dose of therapeutic interest in a reasonable time, more than 10^{10}

Table 8.1 The most important clinical centers for hadron therapy operating in 2011

1990	Loma Linda	USA	Protons	250 MeV
1994	Himac Chiba	JPN	Carbon	800 MeV/u
1994	NCC, Kashiwa	JPN	Protons	235 MeV
2001	HIBMC, Hyogo	JPN	Protons	230 MeV
2001	PMRC, Tsukuba	JPN	Protons	250 MeV
2001	NPTC, MGH, Boston	USA	Protons	235 MeV
2003	Shizuoka	JPN	Protons	235 MeV
2004	MPRI, Bloomington	USA	Protons	200 MeV
2004	WPTC, Zibo	CHN	Protons	230 MeV
2006	MD Anderson Houston	USA	Protons	250 MeV
2006	FPTI, Jacksonville	USA	Protons	230 MeV
2007	NCC, Ilsan	KOR	Protons	230 MeV
2009	ProCure, Oklahoma City	USA	Protons	230 MeV
2009	RPTC, München	GER	Protons	250 MeV
2009	HIT, Heidelberg	GER	Protons, Carbon	430 MeV/u
2010	UPenn, Philadelphia	USA	Protons	230 MeV
2010	CNAO, Pavia	ITA	Protons, Carbon	430 MeV/u
2010	WPE, Essen	GER	Protons	230 MeV
2010	CPO, Orsay	FRA	Protons	230 MeV
2010	PTC, Marburg	GER	Protons, Carbon	430 MeV/u
2010	Gunma, Maebashi	JPN	Protons	400 MeV/u
2010	HUPBTC, Hampton	USA	Protons	230 MeV
2010	SJFH, Peking	CHN	Protons	230 MeV

Source <http://www.klinikum.uni-heidelberg.de/Therapy-centers-in-the-world>

particle/s have to reach the tissue under treatment. None of these performances has been achieved so far with laser techniques. Some of them seem still hard to achieve with existing lasers or even with the new generation lasers, at least in a configuration practically usable in a hospital context. In the following we will consider several options which are currently investigated or could be in the near future with upgraded laser systems.

8.2.2 Laser-Based Ion Acceleration Schemes Suitable for Medical Applications

A high power laser primarily acts with e.m. field on electrons (first bound, then free after ionization), while action on massive particles (protons and ions) needs the intermediate role of these electrons. This scenario has been described in many works after the advent of powerful laser systems and has been recently reviewed within

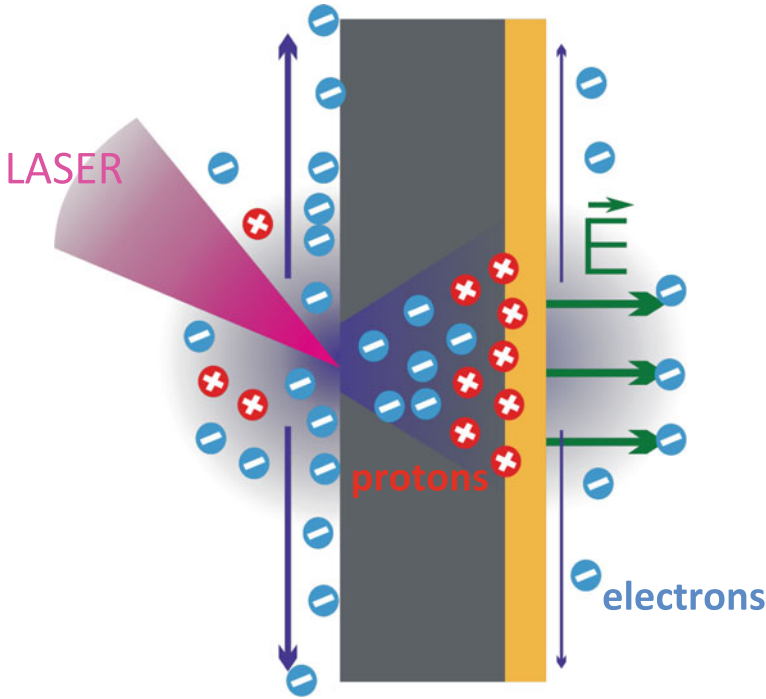


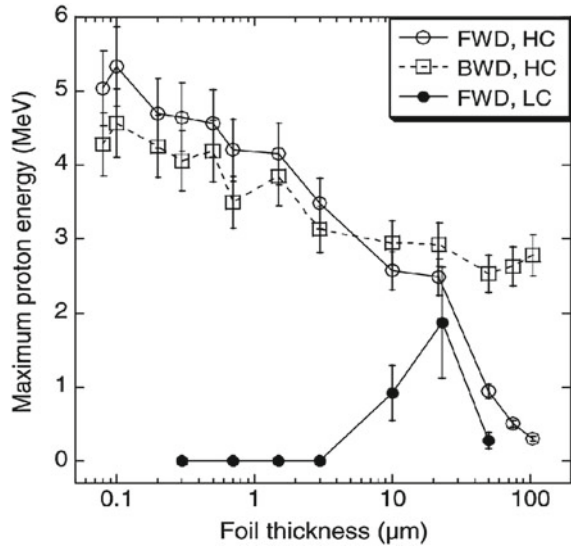
Fig. 8.3 Sketch of laser induced charge dynamics preceding proton acceleration by TNSA

the correct theoretical background by Mulser and Bauer [25]. More recent review papers specifically devoted to laser-driven ion acceleration includes [26, 27], this latter more addressed to applications.

Let's briefly consider here the main schemes currently under study for the acceleration of protons and ions via laser-matter interaction in view of their possible application to the medical purposes, first of all radiotherapy of cancer. We will refer to Fig. 8.3 as a basic geometry involving three physical elements, namely the *laser pulse* focused on a *target* and generating a *proton beam*. Each of the three elements, together with the interaction geometry, will be characterized by a set of parameters whose combination will define the physical regime of interaction and consequently the regime of proton acceleration. Notice that Fig. 8.3 is merely representative and the actual geometry can be considerably different, e.g. available protons could escape also from the opposite side of the target.

In order to be of therapeutic interest the proton (ion) beam has to release more than 10^{10} quasi-monoenergetic particles per second, with a kinetic energy >200 MeV (400 MeV/u). This challenging performances need probably a laser pulse peak power exceeding the PW at a pulse repetition rate of the order of kHz and a high speed target-refreshing system, with a high degree of shot-to-shot reproducibility of

Fig. 8.4 Maximum proton energy versus target thickness for high-contrast (HC) and low-contrast (LC) laser pulses (Ceccotti et al. [31])



the particle beam parameters. Of course a crucial role will be played by the physical processes involved in the acceleration regime.

The *target normal sheath acceleration* (TNSA) regime has been the most studied so far, experimentally, theoretically and numerically. A TNSA model was firstly proposed by Wilks et al. in 2001 [28] to interpret the first experimental observations [29], of high energy protons escaping the rear side of the laser irradiated target [30] like in the sketch Fig. 8.3. This process is described as due to the extremely high electric field generated by many relativistic electrons escaping the rear surface and forming a cloud parallel to that surface.

A rich crop of experimental data basically confirmed the model and enriched it with a number of variants, including laser pulse and target optimization. Target thickness was proved to be a crucial parameter, leading to either higher proton energy with thinner target, provided the *contrast* of the main laser pulse over the *pre-pulse* (see Fig. 8.5) was very high [31], or determining an optimum thickness for a given finite contrast [32], as shown in Fig. 8.4. The data plots also show that with ultra-high contrast and thin foil targets the proton energy has about the same trend for protons coming either from the front or from the rear face [31].

As for a possible accelerator based on thin foils, high repetition rate requested by clinical uses would require sliding tape or similar devices. Another parameter to be exploited is the target size (mass), which led to a series of experiments with “mass-limited” targets. In principle, reducing the target surface should result in a denser electron cloud and higher ion accelerating field. This assumption is well confirmed by numerical simulations but only partially by experiments. High rate injection of such “pellets” would be an additional problem for an accelerator operating at high rep-rate.

Apart for some “exotic” targets or sophisticated configurations [26, 27], proton spectra produced by TNSA show a broad, thermal-like energy spectrum. This feature risks to vanish the advantages of the Bragg peak in deep energy deposition, which is the strongest motivation for hadron therapy. Most of the energy broadening in the TNSA acceleration is due to the initial distribution of protons in a wide region where the accelerating field varies considerably. An effort at designing special targets (e.g. with small dots of proton-rich material on surface or “grating targets” [33]) is currently in progress with a partial but encouraging success. At the same time several kind of passive filters able to reduce the outcoming proton spectrum are tested. It has to be considered, however, that any kind of passive particle filtering will introduce an additive radioactivation trouble in a clinical context.

Given the current limitations of maximum energy and energy spread of TNSA based ion sources, a possible approach consists in the use of hybrid structures including a TNSA based source, acting as an injector, and a post-acceleration assembly to select and boost the energy to the levels needed for clinical tests. In fact, in the TNSA regime, the proton beam is characterized by an exponential energy spectrum, with a cutoff energy and broad angular divergence. Conventional transport lines are being designed [34] to perform energy selection and beam collimation. These transport and selection lines are based on compact solenoid and magnetic quadrupoles. To increase the maximum available energy, injection of protons into a small linac has been proposed for post-acceleration. Realistic start-to-end simulations of these schemes, based on actual TNSA performances, show that this approach may lead to a prompt and profitable exploitation of currently available laser-driven proton and ion sources.

Let’s now consider *radiation pressure dominated acceleration (RPDA)*. Pressure of e.m. radiation on an interface of two media is a classical, non-trivial topic [35] still under investigation [36], including possible applications, ranging from pushing aircrafts to accelerating particles with powerful laser pulses. This latter option has been widely discussed and partially tested experimentally for proton acceleration in the last decade [26, 27]. Without going in detail, we will briefly consider its potential for medical applications, as well as some of its drawbacks. In order to avoid the misleading crop of terms used in the literature, like “hole boring”, “laser piston”, “sweeping effect”, “light sailing”, etc., let us simply distinguish between the two limit cases of thick and thin target, respectively.

In this context, we can consider “thick” a target much thicker than the one for which ion acceleration can occur by the direct space-charge effect. In this condition interpretation of experimental results is quite tricky since the action of the radiation pressure is mixed and somehow confused with the action of the shock wave propagating in the target material. The shock wave in turn can be partially pushed by light pressure at very high irradiance. This scenario is further complicated by the presence of a plasma in front of the target before the arrival of the main laser pulse (pre-plasma), unavoidable with thick targets. All this makes presently difficult to evaluate the potential of thick target technique for medical applications, in spite of a large crop of models and results in a variety of conditions.

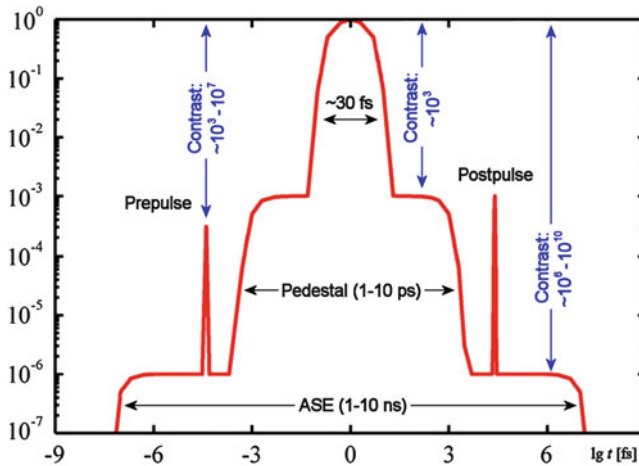


Fig. 8.5 Time evolution of parasitic laser emission before and after the main pulse

The situation is different with “thin” targets, i.e. so thin that the laser pulse *passes through* the target and ions are accelerated *during* the pulse itself. This regime is extremely promising for applications which need ions of very high energy with control of their spectrum. However, for a clear and complete test of the various scaling laws published in the last years, laser intensity $> 10^{23}$ W/cm² is requested. This condition demands then a general upgrading of the existing lasers as discussed in the next paragraph. There are plenty of other possible acceleration mechanisms of ions from ultra-high intensity laser interaction with matter which have been proposed and (some of them) very preliminary tested [26, 27]. Their discussion is out of the purpose of this work. We only observe that this variety of proposals proves that this field is extremely active and productive scientifically, but probably still not mature for practical applications, in particular for the highly demanding clinical application.

As already anticipated above, in most of the laser-based ion acceleration schemes a crucial role is played by the laser *pulse contrast*, more exactly by the ratio between the main pulse peak *power* and the power associated with the light emitted by the laser chain *before* the main pulse itself. In Fig. 8.5 the emitted power versus time is sketched in a log-log diagram. Though all the early emission is often indicated as *prepulse*, the actual prepulse (left hand peak in Fig. 8.5) is an ultrashort pulse, similar to the main pulse but much weaker, leaking from the electro-optical shutter out of the oscillator. This prepulse usually carries a negligible amount of energy (and power). More dangerous is the *amplified spontaneous emission* (ASE), also called *ASE pedestal*, which lasts typically a few nanosecond and then carries a considerable amount of energy, comparable with the main pulse energy if the contrast is worse than 10^6 . In most of the previous experiments on laser-driven proton acceleration the contrast had to be increased to better than 10^9 , with several means, including the “plasma mirror” technique [31, 37]. Early emission a few picosecond before

the main pulse involves the *ps-contrast* which is usually 3–4 orders of magnitude worse than the ASE-contrast, but carries much less energy. This latter can be reduced only assuring high quality and accuracy in the optical compression of the stretched amplified pulse at the end of the laser chain. A critical feature of the pre-pulse problem is that most of the undesired effects depend on the absolute value of the pre-pulse energy and power and not from the value of the contrast. In other words, increasing the laser power, as necessary at increasing the ion energy, the contrast has to be increased correspondingly.

8.2.3 Laser Upgrading to Catch Suitable Ion Beam Energy

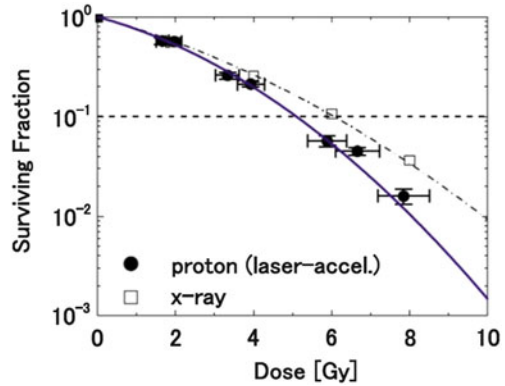
It has been clear for a long time that, differently from electrons (see next sections), proton sources driven by laser need not only high pulse peak intensity but also high energy per pulse. A pioneering experiment from Lawrence Livermore National Laboratory, demonstrated high current proton beams of several tens of MeV's [38] with PW laser pulses whose high contrast was assured by a plasma-mirror technique [37]. Preliminary investigations were performed in many laboratories with femtosecond and picosecond pulses of different power. These investigations were quite useful to assess the validity of various schemes achievable at the available laser fluence but they also evidenced that for getting kinetic energy and mean proton current suitable for clinical application, a general laser upgrading was necessary. Further, a decisive progress of laser technology towards higher peak power, higher contrast (see above), higher repetition rate has to be faced.

As an example, at Kansai Photon Science Institute of JAEA (Japan) an Advanced Beam Technology Division has been created with the purpose of designing a new-concept laser facility able to drive protons to 200 MeV kinetic energy. Previous experimental campaign 2004–2011 at KPSI/JAEA was quite successful. By increasing laser intensity on target from 10^{18} up to 10^{21} W/cm² the maximum proton energy increased progressively from 0.4 upto 40 MeV. This latter however was found to be also an energy limit due to the performances of the existing laser system J-KAREN [39].

The upgrading from J-KAREN to J-KAREN-P, which will deliver multi-PW power, is based on the original J-KAREN technology [40, 41] including OPCPA amplifiers and ultra-high contrast of the output pulse [42].

It is interesting to consider the expected effect of such a laser upgrading on the energy of protons which can be accelerated by focusing the laser pulse up to 10^{22} W/cm² with a contrast $>10^{11}$. Both TNSA and RPD acceleration schemes qualitatively converge towards expectation of proton energy above 200 MeV, also supported by numerical simulations performed for both extended and mass-limited thin foil targets.

Fig. 8.6 Measured rate of survival of cancer cells after irradiation with laser produced protons (0.2 Gy/shot, LET = 18 keV/ μm) with a determined RBE of 1.20 ± 0.11 (Yogo et al. [44])



KPSI/JAEA strategy for producing high energy protons is based on 40 fs laser pulses and consequent choice of acceleration schemes and target thickness and size. Some other labs have a different strategy according to the choice of longer (picosecond) or shorter (≈ 10 fs) laser pulses, respectively. Acceleration mechanisms and targetry will be varied consequently.

8.2.4 Radiobiology with Present Laser-Produced Ion Beams

Though ions produced with laser-plasma techniques are still far from clinical requirements, they are currently used for preliminary tests on biological samples in order to assess their capability as ionizing agent, also considering the ultra-short duration of the laser-produced particle bunches, compared with the ones delivered by RF-based machines. Relatively low kinetic energy, broad energy spectrum and large divergence of the beams do not prevent possibility and interest for such investigations.

Taking into account their high-LET (linear energy transfer), protons of a few MeV have been compared, in terms of relative biological effectiveness (RBE), with both RF-accelerated protons and standard X-ray sources. Yogo et al. have first demonstrated breaking of DNA in human cancerous cells with laser-accelerated protons [43], then measured their RBE [44] as shown in Fig. 8.6. A relevant feature of laser-produced proton bunches lies on their outstanding instantaneous dose rate, due to their duration of about 1 ps, more than one million times shorter than RF-produced pulses. Dose rate as high as 10^9 Gy/s have been obtained and tested on biological samples [45].

In this condition a single laser shot exposure could allow a clonogenic assay on tumor cells which appeared to be in line with previously published results employing RF-driven proton sources. On the other hand, Relative Biological Effectiveness (RBE) was estimated to be of the order of 1.4 at 10 % survival from a comparison with a “standard” 225 kVp X-ray source [45].

Ultra-high dose rate opens investigation of an unexplored regime of radiobiology, where collective effects [46] could add to individual particle effects on the cell, due to the extremely high particle density. On the other hand, ultra-short duration may open the way for studying (e.g. via pump/probe experiments) very early elementary processes occurring at a nanometer scale at the occurrence of the “instantaneous” ionizing action. These early physical and chemical processes are basically unknown. This exciting scientific perspective will be discussed also for ultrashort electron bunches (Sect. 4.2).

All these novel studies have to face a considerable difficulty due to the lack of suitable dosimetry for particle bunches of such a short duration and such a high dose rate. This point is common to laser-driven sources of both hadrons and electrons (Sect. 4.1). Novel devices and methods for dosimetry of ultrafast particle bunches are being proposed and tested recently. Fiorini et al. developed a new procedure [47] including the use of a magnet and Gafchromic films which, after a suitable Monte Carlo treatment of data, can provide both dose and energy spectrum of protons reaching the sample. This sophisticated procedure however needs the application of two correction factors: the first one, to take into account the variation of the dose response of the films as a function of the proton energy, and the other to calculate the dose at the cell layer from the dose measured on the films.

8.2.5 Laser-Driven Ion Microscopy

Ions produced with laser-based techniques can be used for high-resolution ion microscopy (ionography) of biological sample. For this application high kinetic energy of particles is not needed and also sub-MeV ions can produce high quality images provided the sample thickness is below but near the stopping range for the given energy band. It has to be considered that for contact microscopy also a high divergence of the ion beam can be tolerated, provided the spatial distribution of particle on the sample is uniform.

Faenov et al. [48] produced $> 10^{18}$ multicharged carbon and oxygen ions per laser shot by irradiating CO₂ clusters from a gas-jet. The ion energy was measured to be ≥ 300 keV. With such rather divergent but uniform ion beam, ionography of a spider net revealed submicron details, as shown in Fig. 8.7.

8.3 Laser-Driven Electron Acceleration Towards Medical Applications

Starting from the “famous” triple communication of achievement of quasi-monochromatic electron bunches, by ultrashort intense laser interaction with gas-jets, 10 years ago [49–51], soon followed by the GeV achievement [52], an incredible crop of progressive successes has been reported in the scientific literature. Kinetic

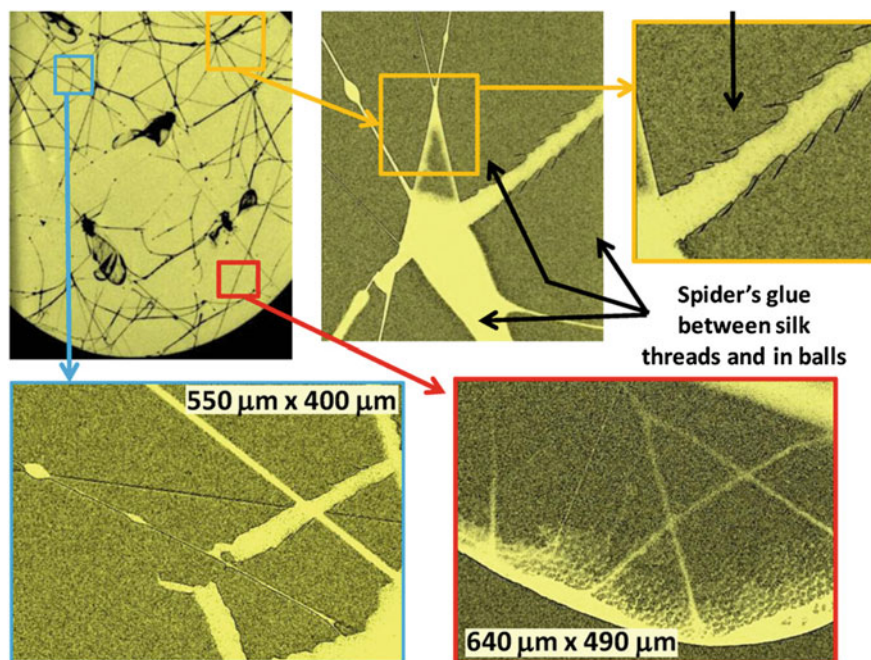


Fig. 8.7 Ion microscopy with carbon and oxygen ions produced by laser interaction with a CO_2 clustered jet: contact image of a spider web and magnified details showing high resolution (Faenov et al. [48])

energy and “quality” of the electron bunches have been enormously increased, in terms of energy control, spectrum narrowing, collimation, pointing stability, reproducibility of the process, by using a variety of targets, mostly gaseous, but also solids, these latter including thin dielectric foils. Recently electron bunches peaked at 2 GeV with only a few per cent energy spread and sub-milliradian divergence were reported [53] by focusing into a pulse-filled He cell a PW laser pulse. Beside these exciting records obtained with such powerful lasers, a great effort is devoted in many laser labs in order to obtain electron bunches suitable for medical applications, first of all radiotherapy of cancer. Since energy suitable to this kind of application ranges from a few up to a few tens of MeV, smaller laser equipment’s are requested, typically a few tens of TW peak power. In principle, this kind of “table top” laser driven electron accelerators (Laser-Linac) are good candidates at competing with RF-based Linac currently used for radiotherapy in hospitals. Suitable kinetic energy and dose delivered in an acceptable treatment time are already available from Laser-Linac’s. However, kinetic energy control, stability and reproducibility of the process have still to be improved in order to match clinical standards. On the other side, the much higher peak-dose-rate (of the order of 10^9 Gy/s) that can be achieved with laser techniques, opens an exciting field of radiobiological investigation with unpredictable consequences for the radiation therapy of tumors.

8.3.1 Present RF-Driven Versus Possible Laser-Driven Devices (Electrons and Photons)

Though the rate of survivals increases regularly year by year, cancer is still the first cause of death everywhere. The number of new cases of cancer in the world are estimated to have been about 13 millions in the year 2010, with an expectation of 20 millions in 2020 [54]. About 50 % of cases are treated with radiation therapies, possibly in combination with surgery and/or chemotherapy, with an emerging problem for the access of low- and middle-income countries (LMIC) to radiation therapy [55].

Among these treatments, more than 90 % use RF-driven linear accelerators of electrons (RF-Linac). Other techniques include internal radiation (brachytherapy) and proton-ion beams. These latter were discussed in the previous Sect. 8.2. In most cases electrons delivered by a RF-linac are not used directly on the tumor but converted into photons (hard X-rays) by bremsstrahlung through a suitable target. In some case electrons are used directly, either to cure superficial tumors or in the Intra-Operative Radiation Therapy (IORT) which can be applied during surgical operation of a tumor [56, 57].

Radiation therapy techniques evolve and progress continuously and so do accelerators and dose delivering devices which share a global market of \$3–4 billions, growing at an annual rate of 5.4 % [58]. Most of the progress involves precision in tumor targeting, multi-beam irradiation, reduction of damage on healthy tissues and critical organs, fractionation of dose delivering for a more effective cure [59]. However, requirements on the electron beams to be suitable to a clinical use remain unchanged and they supply the benchmark for the progress of the laser-based clinical accelerators.

Basically, requested electron kinetic energy ranges from 4 to 25 MeV, but rarely energy above 15 MeV is used. Required dose/rate usually ranges from 1 to 10 Gy/min. These two ranges of performances are presently well fulfilled by plasma accelerators driven by ultrashort laser pulses of “moderate” peak power, i.e. few tens of TW, operating within high efficiency laser-plasma interaction regimes at a pulse repetition rate of the order of 10 Hz [60]. However further work has to be done on laser acceleration in order to reach the clinical standard in terms of the electron output stability and reproducibility.

Several tasks have to be afforded before proceeding to a technical design of a laser-driven linac prototype for clinical tests. A first task is the optimization of both laser and gas-jet (or other possible targets) as well as their coupling (involving mechanical stability and optical design). Another task is the energy control of the electron bunch to provide different electron energies on clinical demand. These goals would require a complex scientific and technological investigation addressed to both the laser system, in order to make it as stable, simple and easy to use as possible and to the physics of the acceleration process, in order to get the highest possible efficiency, stability and output control [61].

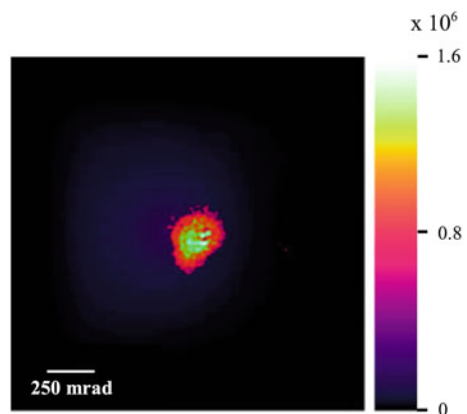
We may nevertheless try and list some of the expected advantages of future Laser-linac's for clinical uses. Laser technology strongly reduces size and complexity of the acceleration section (Mini-linac) of the device; it also totally decouples the “driver” from the acceleration section: we can imagine a single high power laser plant in a dedicated hospital room (with no need for radioprotection) which delivers pulses to a number of accelerators located in several treatment or operating rooms, suitably radioprotected. Laser managing and maintenance can proceed independently from the managing and maintenance of the Mini-linac's. Each Mini-linac could be easily translated and rotated according to the given radiotherapy plan. Current studies (see also Sects. 4.1 and 4.2) could prove that the extreme dose-rate per pulse delivered by the Laser-linac would reduce the total dose for a therapeutical effect. This latter of course would be a major advantage.

8.3.2 High Efficiency Laser-Driven Electron Acceleration to Relativistic Energies

If we limit our consideration to radiotherapy, present table-top laser driven electron accelerators can be already considered as candidate. In fact, for this medical application, most of the requirements usually asked to electron bunches are considerably relaxed. Small divergence, monochromaticity, pointing stability, etc. are requested at a moderate level, while the main effort has to be devoted to efficiency, stability and reliability of the process in order to provide clinically acceptable devices.

As far as the efficiency is concerned, in an experiment performed at CEA-Saclay (France) a regime of electron acceleration of high efficiency was found, using a 10 TW laser and a supersonic jet of Helium [60]. This *table-top* accelerator delivered high-charge (nC), reproducible, fairly collimated, and quasimonochromatic electron bunches, with peak energy in the range 10–45 MeV. In Fig. 8.8 a typical cross

Fig. 8.8 25-MeV electron beam cross section (Giulietti et al. [60])



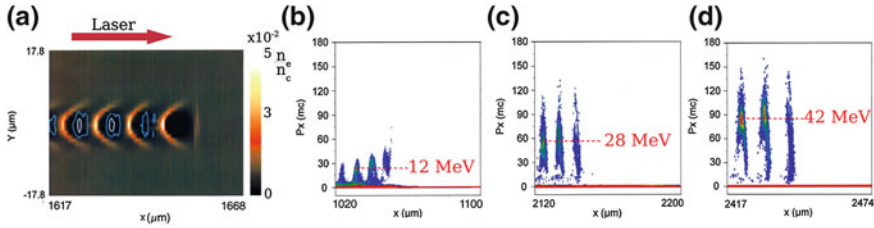


Fig. 8.9 Snapshots from the 3D simulation. **a** Electron density distribution when the laser pulse is at about 1.65 mm after the entrance in the gas jet. **b–d** Electron momentum distribution along the propagation axis when the laser pulse is at 1, 2, and 2.5 mm, respectively (Giuliotti et al. [60])

Table 8.2 Comparison between commercial RF-linac's and experimental Laser-linac

Linac	IORT-NOVAC7	LIAC	Laser-linac (experimental)
Company	(SORDINA SpA)	(Info & Tech Srl)	(CEA-Saclay)
Max electron energy	10 MeV	12 MeV	45 MeV
Available energies	(3, 5, 7, 9 MeV)	(4, 6, 9, 12 MeV)	(5–45 MeV)
Peak current	1.5 mA	1.5 mA	>1.6 KA
Bunch duration	4 μ s	1.2 μ s	<1 ps
Bunch charge	6 nC	1.8 nC	1.6 nC
Repetition rate	5 Hz	5–20 Hz	10 Hz
Mean current	30 nA @5 Hz	18 nA @10 Hz	16 nA @10 Hz
Released en. in 1 min	18 J @ 9 MeV	14 J @ 12 MeV	21 J @ 20 MeV

section of the relativistic electron beam at 25 MeV is shown, after de-convolution of experimental data from the SHEEBA radiochromic film stack device [62].

3D particle-in-cell simulation performed with the numerical code CALDER [63] reveals that the unprecedented efficiency of this accelerator was due to the achievement of a physical regime in which multiple electron bunches are accelerated in the gas-jet plasma during the action of each laser shot. This effect is shown in Fig. 8.9 by the simulation sequence.

With this experiment, laser driven electron acceleration approached the stage of suitability for medical uses, in particular for Intra-Operative Radiation Therapy (IORT) of tumors [56, 57]. Comparison of the main parameters of electron bunches produced by a commercial RF Hospital accelerator for IORT treatment and those of the present laser driven accelerator is shown in the Table 8.2.

In the same experiment electron bunches of ≈ 40 MeV were converted, via bremsstrahlung in a tantalum foil, into gamma rays with a strong component in the range 10–20 MeV, which matches the Giant Dipole Resonance of nuclei. This gamma rays could in turn activate a foil of gold according to the nuclear reaction

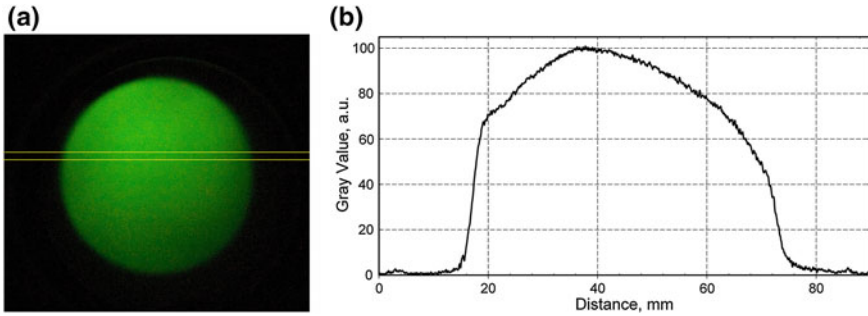


Fig. 8.10 Distribution on sample of electrons from the 300 keV, high-RBE electron source

$^{197}\text{Au}(\gamma, n)^{196}\text{Au}$. The number of radioactive gold atoms produced in this way was measured [1, 60]. This achievement opens the way to table-top laser-driven nuclear physics and production of radio-isotopes for medical uses.

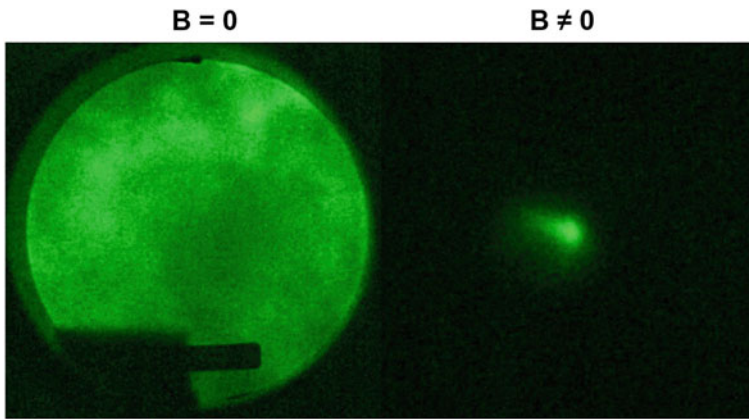
8.3.3 Sub-relativistic Electron Sources

Recently, a laser-driven source of electron bunches with kinetic energy around 300 keV and picosecond duration has been set up at ILIL lab of National Institute of Optics (Pisa, Italy) for radiobiological tests. Each bunch combines high charge with short duration and sub-millimeter range into a record dose rate, exceeding 10^9 Gy/sec. Both high dose rate and the high level of Relative Biological Effectiveness (RBE), attached to sub-MeV electrons, make this source very attractive for radiobiological tests on thin living samples. The source reliability is improved by its shot-to-shot stability and uniform dose distribution on the sample surface, this latter shown in Fig. 8.10. Operating at 10 Hz, the source can deliver high doses in a short exposure time. The physical and radiological performances of the source are indicated in the Table 8.3.

Preliminary tests on biological samples confirm the high performances of the source [64] and its potential for radiobiological studies. In fact, epidemiological and experimental analysis indicates that low-LET (Linear Energy Transfer) radiations (X-rays, electrons) have different RBE's depending on their energy. In particular, higher-energy low-LET radiations are relatively less effective than lower-energy low-LET radiations. In particular, there is a factor of about 3–6 increase in effectiveness in 30 kVp X-rays and for tritium beta rays compared to 15 MeV electrons [65]. On the other hand the limit that low energy radiation is absorbed in a small penetration depth turns out in an increased dose for thin bio-samples.

Table 8.3 Main performances of the ILIL source of sub-relativistic electrons

Number of electrons N_e per bunch	$N_e \approx 10^{10}$
Bunch duration on sample	≈ 3.5 ps
Bunch length L	$L \approx 1$ mm
Kinetic energy (E) distribution	Approx. Maxwellian $\approx \exp[-E/kT]$
Source temperature T	$T \approx 300$ keV
Stopping power in water ($E = 300$ keV)	2.36 MeVcm ² /g
Range in water ($E = 300$ keV)	0.84 mm
Dose released by each bunch in water	3.5 mGy
Dose rate in water during the bunch	10^9 Gy/s
Bunch repetition rate	10 Hz
Multi-bunch dose rate	35 mG/s
Time for delivering 1 Gy	≈ 30 s

**Fig. 8.11** Collimation effect of external magnetic field

Such sub-relativistic electron beams can be also easily focused by an external magnetic field in case the irradiation has to be confined in a small area of the sample. Recently, several magnetic field configurations have been successfully tested in order to find the optimum focusing on sample for an electron beam of 300 keV [66]. Figure 8.11 clearly shows that, with a suitable magnetic configuration, even an initially non-uniform electron beam can be strongly focused on the sample position. The same work also proved that the magnetic field can be beneficial also in stabilizing the electron beam pointing on a given target spot.

8.4 Radiological Use of Electron Bunches from Laser-Plasmas

8.4.1 Ionizing Electron Bunches for Biological Tests and Advanced Dosimetry

As of today, the basic ionizing radiation used in cancer radiotherapy is represented by X-rays and electron beams in the energy range of 4–25 MeV. Nevertheless, new irradiation sources based on laser-plasma accelerated electrons are now emerging, characterized by ultra-short particle bunches (\sim ps) and ultra-high dose rate that could result in peculiar radiobiological properties [67]. In order to be actively used in the future for cancer radiotherapy, laser-plasma electron sources have to meet requirements as efficiency, long-term stability, reproducibility and reliability of the process in order to provide clinically acceptable devices. Moreover, sufficient particle intensities and controlled delivery of the prescribed dose at the treatment site has to be assessed [68].

Radiological use of laser-plasma accelerated electrons implies a well-defined dosimetric characterization. Apart from retrospective precise dose determination and dose homogeneity control by means of Faraday cup and GafChromic films, Monte Carlo simulations performed with the code GEANT4 have allowed the “a priori” characterization of dosimetric properties of relativistic electron beams produced in laser-plasma acceleration. Figure 8.12 shows the simulated dose deposited by a 6 MeV electron bunch at various depths inside a water phantom [69].

Following the translational research chain from bench to bedside, the laser based technology was developed for cell irradiation experiments as the first translational step. Its stable and reliable application was proven in systematic radiobiological studies like the one performed at Friedrich Schiller University with the JETI laser system [70]. Tumor and non-malignant cells were irradiated with pulsed laser-accelerated electrons in the range 3–20 MeV for the comparison with electrons of a conventional Linac for therapy. Dose response curves were measured for the biological endpoints, clonogenic survival and residual DNA double strand breaks. The overall results show no significant differences in radiobiological response for in vitro cell experiments

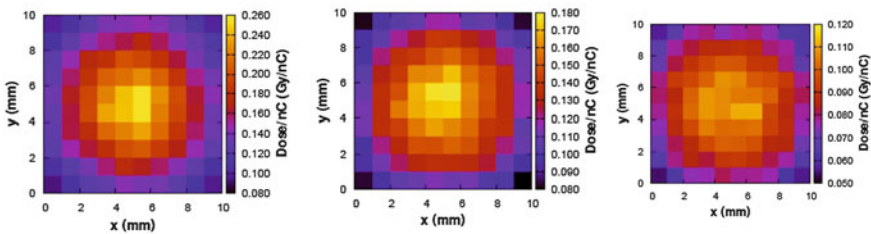


Fig. 8.12 2D maps of the dose deposited by e⁻ at 0.5, 4.5 and 9.5 mm depth (Labate et al. [69])

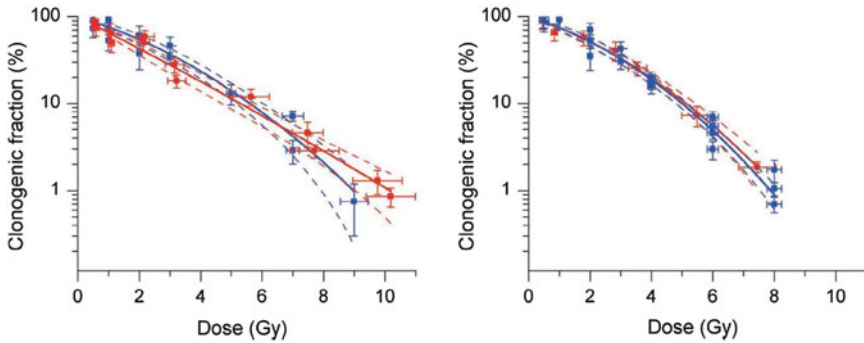


Fig. 8.13 Dose response curves of clonogenic survival after irradiation of normal tissue cell line 184A1 (*left*) as well as tumor cell line FaDu (*right*) with pulsed laser generated electron beam (*red curves*) and continuous electron beam delivered by a therapeutic LINAC (*blue curves*). All curves are presented in consideration of their 95 % confidence intervals (Laschinsky et al. [70])

between laser and RF produced electron beams, suggesting that no systematic difference exists between the two sources. Figure 8.13 shows dose response curves of clonogenic survival after irradiation with pulsed laser generated electron beam and continuous electron beam delivered by a therapeutic LINAC.

Similar experiments have been conducted on cell monolayer and lymphocytes at ILIL-INO laboratory of the National Research Council in Pisa, using a 2 TW Ti:Sa laser and accelerated electron in the range 5–20 MeV. The electron bunches have been fully characterized, in terms of spectrum, divergence and total charge, using GAFChromic Films (GAF) packed in a stack and separated by solid water, and GEANT4 library has been used to retrieve the dose delivered to the biological samples. DNA double-strand breaks (DSB) and nucleo-cytoplasmic translocation alterations have been inspected as biological endpoint [71].

Animal experiments have been carried out at Friedrich Schiller University, proving the feasibility of a laser based irradiation system with all key components as beam transport system, real-time beam monitoring, absolute dosimetry and reproducible positioning of the tumor on beam axis [72]. However, new insights into completely unexplored domains as cell and tissue responses to pulsed ultra-high dosed rates may also be provided by ultra-fast spatio-temporal radiation biology and dosimetry.

8.4.2 “Femto-Nano” Scale Radiobiology

Conventional radiobiology studies and measures the effects of ionizing radiation on living cells, mostly considering cell death and apoptosis, DNA damage and repair, recombination, and mutagenesis. In addition, there is research on the role of oncogenes in cancer, RNA processing in eukaryotes and radiobiology topics related to cancer therapy. All these observations and measurements usually lie on a time scale ranging from few minutes to several days.

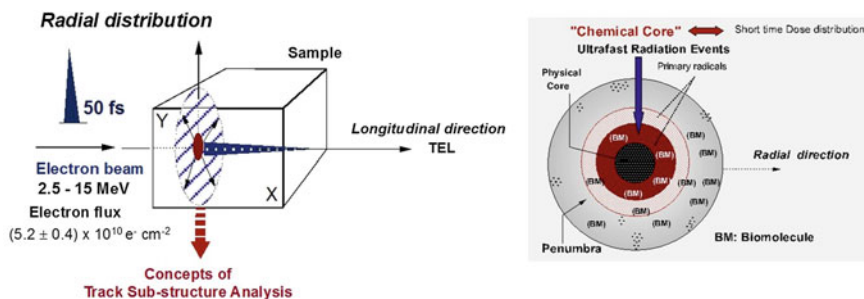


Fig. 8.14 Basic layout of High Energy Radiation Femtochemistry (HERF) concept. Courtesy of Y. Gauduel

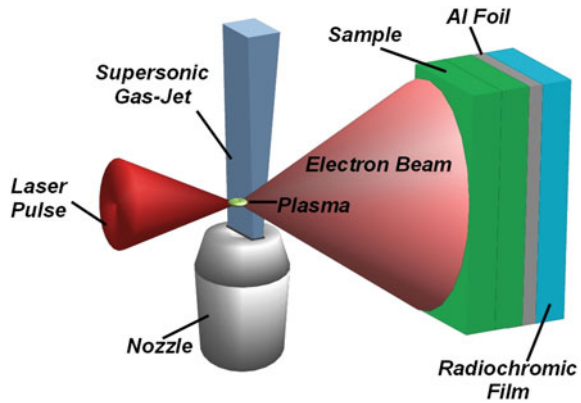
Early deposition of energy and energy spreading in a cascade process is usually described by Monte Carlo code simulations but very few is known about the “instantaneous” response of the components of a living cell at this early stage. On the other hand, the early profile of energy deposition is decisive for the prediction and control of radiation-induced biomolecular and sub-cellular damage, and consequently for cancer therapy protocols. This point could become of extreme relevance if ultra-short, laser driven, ionizing pulses of radiation/particles will be used in the future radiotherapy.

That’s why recently a novel approach to radiation biology has been proposed [73, 74] for the complete understanding of biophysical events triggered by an initial energy deposition inside confined ionization clusters (tracks) and evolving over several orders of magnitude, typically from femtosecond and sub-nanometer scales up to the scale of conventional radiobiology. To this purpose, femtosecond laser sources providing ultra-short pulses of both optical photons and relativistic electrons, in the eV and MeV domain respectively, open exciting opportunities for a real-time imaging of radiation-induced biomolecular alterations in nanoscopic tracks. Figure 8.14 shows the basic spatio-temporal geometry of this approach.

Recently, using a very short-lived quantum probe (2p-like excited electron) and high-time resolved laser spectroscopic methods in the near IR and the temporal window 500–5000 fs, Gauduel et al. could demonstrate that short-range coherent interactions between the quantum probe and a small biosensor of 20 atoms (disulfide molecule) are characterized by an effective reaction radius of ≈ 1 nm. For the first time, femtobioradical investigations performed with aqueous environments gave correlated information on spatial and temporal biomolecular damages triggered by a very short lived quantum scalpel whose gyration radius is around 0.6 nm [16].

There is the hope that this innovating approach would be applied to more complex biological architectures such as nucleosomes, healthy and tumor cells. In the framework of high-quality ultra-short penetrating radiation beams devoted to pulsed radiotherapy of cancers, this concept would foreshadow the development of real-time nanobiodosimetry combined to highly-selective targeted pro-drug activation.

Fig. 8.15 Basic setup for laser-driven electron radiography



8.4.3 Laser-Driven Electron Radiography

Techniques for innovative imaging using electrons represent an important non destructive tool for material science, biology and medicine [75]. Though the use of the laser plasma based electron accelerators for electron radiography is only at the beginning, it can be considered one of the most promising approaches for good quality imaging with particle beams obtainable with miniaturized equipment compared with standard accelerators [73]. Presently, there are only few examples of application of this technique in the field of particle radiography, one of which with laser-produced ions as described in Sect. 2.4 above [48], another with electrons, but generated with conventional linear accelerators [76]. Actually, laser-based accelerators can produce electron beams with enough energy that can penetrate also in dense material [75] and they are certainly an attractive source for probing solid objects on a large area (several squared centimeters). Moreover the compactness of table-top laser accelerators, compared with conventional accelerators, makes this kind of radiography much easier.

The setup is typical of a laser-plasma accelerator: a multi-TW femtosecond laser beam is focused on a gas jet, producing high energy electrons, as shown in Fig. 8.15. Particularly effective is the use of clustered gas jet [77, 78]. In the following example [79] high pressure Argon was released in the pulsed gas-jet, in condition of strong clusterization. The laser was a 2-TW Ti:Sapphire. In this way high charge electron bunches were obtained with a uniform distribution of electrons on the sample, similarly the one shown in Fig. 8.12. About 30 laser shots were enough to obtain a good quality electron radiography.

A typical sample (about 8×5 cm) is shown in Fig. 8.16 left side. In particular this sample included both inorganic and organic elements to test the capabilities of the system in generating radiography. The samples are placed at about 10 cm from the gas jet and, just after the sample, in direct contact, two radiochromic dosimetry films are inserted (Fig. 8.15).

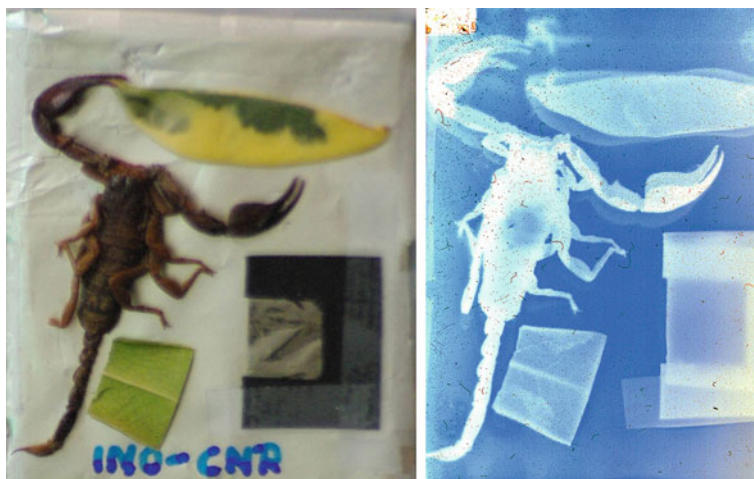


Fig. 8.16 The sample (*left*) and its own electron radiograph. Overall size 35 mm x 48 mm (Bussolino et al. [77])

The possibility of radiographic images generation is proved in Fig. 8.16 right hand side. The image shows detailed features for all elements (inorganic and organic, thin and thick) inserted in the sample, with high contrast. The resolution of the radiography shown in Fig. 8.16 has been estimated to be $\leq 60 \mu\text{m}$, higher than the one obtained in previous works [76, 80]. Simple optical calculations show that with this setup the resolution can be further improved down to $10 \mu\text{m}$ [79].

Transmission electron radiography of organic and inorganic dense objects over a field of view more than 50 mm wide could be easily achieved. The images show details of both thicker and thinner features. The spatial resolution in the current geometrical configuration was limited by geometrical effects combined with the intrinsic detector resolution and scattering from the sample. These results suggest that the availability of a new laser-driven electron source could be taken into account as a substitute to conventional RF electron guns for a cost effective approach to high resolution transmission electron microscopy at high electron energy and for configurations where multiple plasma sources are needed.

8.5 Conclusions

Ultra-short intense laser science has been providing a new class of plasma sources which deliver high energy particles. These sources are candidate at competing with the existing Radio-Frequency driven particle accelerators for many applications, including radiography, radiobiology, radiotherapy and nuclear medicine. Unique features of these novel sources are the reduced size of the accelerating device and the

much shorter duration of the particle bunches. This latter feature can allow ultrafast imaging in radiology, investigation of very early precursors of the biological response and ultra-high peak dose rate in the radiological cure of cancer.

As long as the achievement of clinical standard is concerned, the status of the art is quite different for the laser-driven proton/ion acceleration respect to electron acceleration. Laser-plasma accelerators can easily produce electrons of the requested kinetic energy and deliver the requested dose in a typical treatment time. However they still need to be improved in order to provide the requested electron energy control, as well as the necessary degree of stability and reliability of the acceleration process.

Laser-based proton and light ion acceleration did not reach so far the clinical request in terms of kinetic energy, the necessarily narrow energy spectrum nor the minimum dose rate. Nevertheless the technique is expected to face a decisive improvement when the current upgrading of the laser systems devoted to it will be completed. Each of these upgrading effort is aimed to match a particular acceleration regime among several promising regimes designed by theoretical and numerical calculations. To this respect, the physical investigation is quite active due to the high value of any progress towards the clinical application. In fact, if successful, laser-driven ion accelerators could widely expand the number of hadron-therapy treatments, presently limited by the size and cost of RF-based infrastructures.

At meantime a large crop of data is being currently collected from radiobiological experiments performed with both electron and ion sources based on laser-plasmas on living samples. This novel and challenging investigation will provide the necessary background for the future use of laser based clinical devices in terms of (presently unknown) biological response and ad hoc dosimetry.

Acknowledgments The authors of this Chapter are operating in the framework of the CNR High Field Photonics Unit (MD.P03.034). They acknowledge financial support from the CNR funded Italian research Network ‘ELI-Italy (Attoseconds)’, from the Italian Ministry of Health funded project GR-2009-1608935 (D.I. AgeNaS) and from the INFN funded “G-RESIST” project.

References

1. O. Graydon, *Nature Photonics* **7**, 585 (2013), A. Giulietti and A. Gamucci, *Progress in Ultrafast Intense Laser Science*, Vol. V, Ch. 8, Springer Series in Chemical Physics (Springer, Heidelberg, 2010)
2. G.A. Mourou, T. Tajima, S. Bulanov, *Rev. Modern Phys.* **78**, 309 (2006)
3. S.P. Le Blanc, R. Sauerbrey, S.C. Rae, K. Burnett, *J. Opt. Soc. Am. B* **10**, 1801 (1993)
4. D. Giulietti et al., *Phys. Rev. Lett.* **79**, 3194 (1997)
5. J.K. Koga, N. Naumova, M. Kando, L.N. Tsintsadze, K. Nakajima, S.V. Bulanov, H. Dewa, H. Kotaki, T. Tajima, *Phys. Plasmas* **7**, 5223 (2000)
6. A. Giulietti, P. Tomassini, M. Galimberti, D. Giulietti, L.A. Gizzi, P. Koester, L. Labate, T. Ceccotti, P. D’Oliveira, T. Auguste, P. Monot, Ph Martin, *Phys. Plasmas* **13**, 093103 (2006)
7. A. Giulietti, A. André, S. Dobosz, Dufrenoy, D. Giulietti, T. Hosokai, P. Koester, H. Kotaki, L. Labate, T. Levato, R. Nuter, N. C. Pathak, P. Monot, and L. A. Gizzi. *Phys. Plasmas* **20**, 082307 (2013)

8. T. Tajima, J. Dawson, Phys. Rev. Lett. **43**, 267 (1979)
9. D. Strickland, G. Mourou, Opt. Commun. **56**, 219 (1985)
10. W. Friedhorsky, D. Lier, R. Day, D. Gerke, Phys. Rev. Lett. **47**, 1661 (1981)
11. D.M. Villeneuve, G.D. Enright, M.C. Richardson, Phys. Rev. A **27**, 2656 (1983)
12. V. I. Veksler, in *Proceedings of CERN Symposium on High Energy Accelerators and Pion Physics*, vol. 1, p. 80 (Geneva, Switzerland, 1956)
13. A.P. Fews, P.A. Norreys, F.N. Beg, A.R. Bel, A.R. Dangor, C.N. Danson, P. Lee, S.J. Rose, Phys. Rev. Lett. **73**, 1801 (1994)
14. S. Bulanov, T. Esirkepov, V. Khoroshkov, A. Kuznetsov, F. Pegoraro, Phys. Lett. A **299**, 240 (2002)
15. S.S. Bulanov et al., Med. Phys. **35**, 1770 (2008)
16. Y.A. Gauduel, V. Malka, *Proceedings of SPIE* 8954; doi:[10.1117/12.2038983](https://doi.org/10.1117/12.2038983) (2014)
17. V. Malka et al., Med. Phys. **31**, 1587 (2004)
18. <http://www.cnao.it/index.php/en/>
19. <http://neurosurgery.mgh.harvard.edu/protonbeam/nptcbrochure.pdf>
20. R.R. Wilson, Radiology **47**, 487 (1946)
21. J. Lawrence, Cancer **10**, 795 (1957)
22. S. Sawada, Nucl. Phys. A **834**, 701 (2010)
23. M. Goitein, A.J. Lomax, E.S. Pedroni, Phys. Today **55**, 45 (2012)
24. M. Schippers, *Beam Delivery System for Particle Therapy*, in *Proton and Ion Carbon Therapy*, C.-M. Charlie Ma, T. Lomax (eds.), CRC Press (Boca Raton, FL) p. 43 (2013)
25. P. Mulser and D. Bauer, *High Power Laser-Matter Interaction*, Springer Tracts in Modern Physics, vol. 238 (Springer, New York, 2010)
26. A. Macchi, M. Borghesi, M. Passoni, Rev. Mod. Phys. **85**, 751 (2013)
27. H. Daido, M. Nishiuchi, A.S. Pirozhkov, Rep. Prog. Phys. **75**, 056401 (2012)
28. S.C. Wilks et al., Phys. Plasmas **8**, 542 (2001)
29. Mackinnon et al., Phys. Rev. Lett. **86**(1769) (2001)
30. Zeil et al., New J. Phys. **12**(045015) (2010)
31. T. Ceccotti et al., Phys. Rev. Lett. **99**, 185002 (2007)
32. M. Kaluza et al., Phys. Rev. Lett. **93**, 045003 (2004)
33. T. Ceccotti et al., Phys. Rev. Lett. **111**, 18501 (2013)
34. S. Sinigardi et al., Nucl. Instr. Meth. Phys. Res. **A740**, 99 (2014)
35. L. Landau et E. Lifchitz, *Théorie du Champ*, Editions (MIR, Moscou, 1966)
36. M. Tamburini et al., New J. Phys. **12**, 123005 (2010)
37. M.D. Perry et al., Opt. Lett. **24**, 160 (1999)
38. R.A. Snavely et al., Phys. Rev. Lett. **85**, 2945 (2000)
39. M. Aoyama et al., Opt. Lett. **28**, 1594 (2003)
40. H. Kiriya et al., Opt. Comm. **282**, 625 (2009)
41. H. Kiriya et al., Opt. Lett. **35**, 1497 (2010)
42. K. Ogura et al., Opt. Lett. **37**, 2868 (2012)
43. A. Yogo et al., Appl. Phys. Lett. **94**, 181502 (2009)
44. A. Yogo et al., Appl. Phys. Lett. **98**, 053701 (2011)
45. D. Doria et al., AIP Adv. **2**, 011209 (2012)
46. E. Fourkal et al., Phys. Med. Biol. **56**, 3123 (2011)
47. F. Fiorini et al., Phys. Med. Biol. **56**, 6969 (2011)
48. A.Y. Faenov et al., Appl. Phys. Lett. **95**, 101107 (2009)
49. P.D. Mangles et al., Nature **431**, 535 (2004)
50. G.C.R. Geddes et al., Nature **431**, 538 (2004)
51. J. Faure et al., Nature **431**, 541 (2004)
52. W. Leemans et al., Nat. Phys. **2**, 696 (2006)
53. X. Wang et al., Nature Commun. **4**, Article no. 1988 (2013) doi:[10.1038/ncomms2988](https://doi.org/10.1038/ncomms2988)
54. IARC, Cancer Fact Sheets, Globocan, <http://globocan.iarc.fr/>
55. D. Rodin et al., Lancet Oncol. **15**, 378 (2014)
56. U. Veronesi et al., Ann. Oncol. **12**, 997 (2001)

57. A.S. Beddar et al., *Med. Phys.* **33**, 1476 (2006)
58. <http://www.businesswire.com/news/home/20140313005577/en/Research-Markets-External-Beam-Radiation-Therapy-Devices>
59. R. Baskar et al., *Int. J. Med. Sci.* **9**, 193 (2012)
60. A. Giuliotti et al., *Phys. Rev. Lett.* **101**, 105002 (2008)
61. F. Baffigi et al., The LEARC Concept: Laser-driven Electron Accelerator for Radiotherapy of Cancer, INO-CNR Internal Report (2014). Accessed: ilil.ino.it
62. M. Galimberti et al., *Rev. Sci. Instrum.* **76**, 053303 (2005)
63. E. Lefebvre et al., *Nucl. Fus.* **43**, 629 (2003)
64. L. Fulgentini et al., High RBE doses delivered by a laser driven electron source , INO-CNR Internal Report (2014). Accessed: ilil.ino.it
65. N. Hunter, C.R. Muirhead, *J. Radiol. Prot.* **29**, 5 (2009)
66. Y. Oishi et al., *Jpn. J. Appl. Phys.* **53**, 092702 (2014)
67. V. Malka, J. Faure, Y.A. Gauduel, *Mutat. Res.* **704**, 142 (2010)
68. E. Beyreuther et al., *Med. Phys.* **37**, 1392 (2010)
69. L. Labate et al, INO-CNR Internal Report (prot. 151, 13/01/11) (2011)
70. L. Laschinsky et al., *J. Radiat. Res.* **53**, 395 (2012)
71. L. Labate et al., *Proc.SPIE* **8779** (2013)
72. M. Schurer et al., *Biomed. Tech.* **57**, 62–65 (2012)
73. Y.A. Gauduel et al., *Nat. Phys.* **4**, 447 (2008)
74. Y.A. Gauduel et al., *Eur. Phys. J. D* **4**, 121 (2010)
75. S.P.D. Mangles et al., *Laser Part. Beams* **24**, 185–190 (2006)
76. F. Merrill et al., Electron radiography. *Nucl. Instrum. Method Phys. Res.* **B261**, 382–386 (2007)
77. A.Ya. Faenov et al., *Laser Part. Beams* **26**, 69 (2008)
78. P. Koester et al., *Laser Part. Beams* **33**, 331 (2015)
79. G.C. Bussolino et al., *J. Phys D: Appl. Phys.* **46**, 245501 (2013)
80. V. Ramanathan et al., *Phys. Rev. Special Topics Accel. Beams* **13**, 104701 (2010)